Oikos

OIK-07059

Le Moullec, M., Sandal, L., Grøtan, V., Buchwal, A. and Bremset Hansen, B. 2020. Climate synchronises shrub growth across a high-arctic archipelago: contrasting implications of summer and winter warming. – Oikos doi:10.1111/oik.07059

Appendix 1

Methodological description of average regional synchrony non-parametric bootstrap

Appendix 2

Appendix 1.

Methodological description of average regional synchrony non-parametric bootstrap.

We evaluated the statistical significance of Svalbard July temperature's contribution to the regional average synchrony using a non-parametric bootstrap. For this, we randomly resampled years of observed ring growth values from pairs of sites and the corresponding climate variables (i.e. July temperature, linearly detrended for the length of the site's specific ring growth time-series). Resampling was done with replacement for the length of overlap between the two time-series of a pair of sites. The correlation coefficient between a pair of sites i and j (ρ_{ij}) was calculated with the corresponding resampled years. Similarly, we computed the correlation coefficient between pairs of sites after accounting for the corresponding resampled time-series of July temperature (i.e. residuals extracted from a linear model, ρ_{res_ij}). Then, the mean correlations over all sites ($\overline{\rho_k}$ and $\overline{\rho_{res\_k}}$ with n = 136 pairwise sites, see Eq. A2 and A4 below) was calculated and we repeated this exercise for m = 1000 iterations. Finally we used the grand mean of these as our estimate of regional average synchrony ($\overline{\rho}$ and $\overline{\rho_{res}}$, see Eq. A1 and A3 below) and the 2.5% and 97.5% quantiles as the 95% confidence interval. Populations were considered to be significantly synchronised if the 95 % confidence interval of the difference in these non-parametric bootstrap distributions (ρ_{diff_k}, see Eq. A5 below, giving a distribution of the differences) did not include zero. Thus,

$$\overline{\rho} = \frac{\sum_1^m(\overline{\rho_k})}{m} \quad \text{(A1)}, \quad \text{where} \quad \overline{\rho_k} = \frac{\sum_1^n(\rho_{ij})}{n} \quad \text{(A2)}.$$

Similarly,

$$\overline{\rho_{res}} = \frac{\sum_1^m(\overline{\rho_{res\_k}})}{m} \quad \text{(A3)}, \quad \text{where} \quad \overline{\rho_{res\_k}} = \frac{\sum_1^n(\rho_{res\_ij})}{n} \text{ (A4)}.$$

Thereafter,

$$\overline{\rho_{diff}} = \frac{\sum_1^m(\rho_{diff\_k})}{m} \quad \text{(A5)}, \quad \text{where} \quad \rho_{diff\_k} = \overline{\rho_k} - \overline{\rho_{res\_k}} \quad \text{(A6)}.$$

Note that the non-parametric bootstrap implemented in the function 'Sncf' from the R package 'ncf' (Bjørnstad 2019) also resamples across years with replacement, but not for a specific pair of sites i and j at a time. Instead, within each iteration, all pairs of sites have the same resampled years.

Appendix 2.

Table A1. Weather station data from across Svalbard with coordinates, time-span and index number corresponding to their map locations in Figure 1. The data was obtained from http://eklima.met.no, except for data from the Hornsund station (Polish Polar Station Hornsund), and data from Barentsburg during the period 1973-1993 and 2004-2014 (<www.tutiempo.net/en/Climate/BARENCBURG/07-1973/201070.htm>). Weather station names in bold represent the six ones with time-series that were long and complete enough to be included in the analysis of spatial synchrony in weather. The superscript '^{P}' indicates weather stations collecting precipitation information.

Station	Latitude	Longitude	Time-span	Map indexing
Akseløya	77.69	14.78	2011-2014	1
Barentsburg^{P}	**78.05**	**14.23**	**1973-1993 and 2004-2014**	**2**
Crozierpynten	79.92	16.84	2010-2014	3
Edgeøya (Kapp Heugelin)	78.25	22.82	2007-2008 and 2011-2014	4
Edgeøya (Svarttangen)	77.53	20.83	2011-2012	5
Hopen^{P}	**76.51**	**25.01**	**1947-2014**	**6**
Hornsund Station^{P}	**77.00**	**15.54**	**1979-2014**	**7**
Isfjord Radio^{P}	78.06	13.62	1947-2014	8
Kongsøya	78.91	28.89	2012-2014	9
Kvitøya	80.11	31.46	2012-2014	10
Longyearbyen^{P}	78.22	15.63	1957-1975	11
Ny-Ålesund^{P}	**78.92**	**11.93**	**1969-2014**	**12**
Pyramiden	78.66	16.36	2013-2014	13
Svalbard Lufthavn^{P}	**78.25**	**15.5**	**1975-2014**	**14**
Sveagruva^{P}	**77.9**	**16.72**	**1978-2014**	**15**
Sørkappøya	76.48	16.55	2011-2014	16
Verlegenhuken	80.6	16.25	2007 and 2011-2014	17

Table A2. List of all variants of the 'Svalbard model' tested, using the function 'dredge' from the R package 'MuMIn' (Barton 2013). All combinations were tested and ranked based on the

parsimony principle of the corrected Akaike information criteron (AICc), using a maximum likelihood approach. RWIt-1= Previous year's RWI, T°C= July mean temperature (°C), Precip.= July precipitation sum (mm), Snow= November-April snowfall amount (mm), log(ROS)="rain-on-snow" in November-April rain sum (mm) on the logarithmic scale, Spring onset= Julian day of spring onset.

Predictors	**df**	**AICc**	**delta**
RWIt-1 + T°C	5	3833.193	0
RWIt-1 + Precip. + T°C	6	3834.85	1.656929
RWIt-1 + T°C + Spring onset	6	3834.999	1.805651
RWIt-1 + Snow + T°C	6	3835.015	1.821144
RWIt-1 + ROS + T°C	6	3835.194	2.000603
RWIt-1 + Precip. + T°C + Spring onset	7	3836.571	3.377155
RWIt-1 + Precip. + Snow + T°C	7	3836.723	3.52931
RWIt-1 + Snow + T°C + Spring onset	7	3836.855	3.661609
RWIt-1 + Precip. + ROS + T°C	7	3836.859	3.665317
RWIt-1 + ROS + T°C + Spring onset	7	3836.963	3.769214
RWIt-1 + ROS + Snow + T°C	7	3837.012	3.818682
RWIt-1 + Precip. + Snow + T°C + Spring onset	8	3838.484	5.291034
RWIt-1 + Precip. + ROS + T°C + Spring onset	8	3838.583	5.389602
RWIt-1 + Precip. + ROS + Snow +T°C	8	3838.736	5.542961
RWIt-1 + ROS + Snow + T°C + Spring onset	8	3838.815	5.622079
RWIt-1 + Precip. + ROS + Snow + T°C + Spring onset	9	3840.496	7.302923
RWIt-1	4	3844.033	10.83975
RWIt-1 + Spring onset	5	3844.855	11.66168
RWIt-1 + Precip.	5	3845.642	12.44897
RWIt-1 + ROS	5	3845.937	12.7433
RWIt-1 + Snow	5	3845.943	12.74924
RWIt-1 + Precip. + Spring onset	6	3846.235	13.0416
RWIt-1 + ROS + Spring onset	6	3846.507	13.31375
RWIt-1 + Snow + Spring onset	6	3846.804	13.6104
RWIt-1 + Precip. + Snow	6	3847.598	14.40494
RWIt-1 + Precip. + ROS	6	3847.632	14.43811
RWIt-1 + ROS + Snow	6	3847.843	14.6495
RWIt-1 + Precip. + ROS + Spring onset	7	3848.086	14.89288
RWIt-1 + Precip. + Snow + Spring onset	7	3848.229	15.03577
RWIt-1 + ROS + Snow + Spring onset	7	3848.455	15.26115
RWIt-1 + Precip. + ROS + Snow	7	3849.584	16.39087
RWIt-1 + Precip. + ROS + Snow + Spring onset	8	3850.076	16.88254
T°C	4	3877.802	44.60849
Precip. + T°C	5	3879.292	46.09835
T°C + Spring onset	5	3879.607	46.41322
Snow + T°C	5	3879.661	46.4676
ROS + T°C	5	3879.752	46.55874
Precip. + T°C + Spring onset	6	3880.99	47.79658

Precip. + Snow + T°C	6	3881.208	48.01421
Precip. + ROS + T°C	6	3881.301	48.10798
ROS + T°C + Spring onset	6	3881.483	48.28981
Snow + T°C + Spring onset	6	3881.494	48.30101
ROS + Snow + T°C	6	3881.604	48.41092
Precip. + Snow + T°C + Spring onset	7	3882.939	49.7458
Precip. + ROS + T°C + Spring onset	7	3882.975	49.78177
Precip. + ROS + Snow + T°C	7	3883.216	50.02301
ROS + Snow + T°C + Spring onset	7	3883.367	50.17314
Precip. + ROS + Snow + T°C + Spring onset	8	3884.921	51.72736
(Intercept only)	3	3889.542	56.34907
Spring onset	4	3890.33	57.13678
Precip.	4	3890.994	57.80062
ROS	4	3891.362	58.16874
Snow	4	3891.474	58.28049
Precip. + Spring onset	5	3891.502	58.30889
ROS + Spring onset	5	3891.823	58.62986
Snow + Spring onset	5	3892.292	59.09862
Precip. + ROS	5	3892.952	59.7582
Precip. + Snow	5	3892.974	59.78013
Precip. + ROS + Spring onset	6	3893.27	60.07647
ROS + Snow	5	3893.292	60.09839
Precip. + Snow + Spring onset	6	3893.507	60.31368
ROS + Snow + Spring onset	6	3893.786	60.59277
Precip. + ROS + Snow	6	3894.928	61.73446
Precip. + ROS + Snow+ Spring onset	7	3895.272	62.07881

Table A3. List of all variants of the 'regional scale model' tested, using the function 'dredge' from the R package 'MuMIn' (Barton 2013). Here, we allowed for among site variations by including an interaction between site and the proposed predictors. All combinations were tested and ranked based on the parsimony principle of the corrected Akaike information criteron (AICc), using a maximum likelihood approach. RWIt-1= Previous year's RWI, T°C= July mean temperature (°C), Precip.= July precipitation sum (mm), Snow= November-April snowfall amount (mm), log(ROS)="rain-on-snow" in November-April rain sum (mm) on the logarithmic scale, Spring onset= Julian day of spring onset.

Predictors	**df**	**AICc**	**delta**
RWIt-1 + ROS + site + T°C + RWIt-1x site + ROS × site	27	3812.771	0
RWIt-1 + site + T°C + RWIt-1x site	19	3816.651	3.879737
RWIt-1 + site + T°C + RWIt-1x site + Precip.	20	3818.108	5.336546
RWIt-1 + site + T°C + RWIt-1x site + Snow	20	3818.487	5.716234
RWIt-1 + site + T°C + RWIt-1x site + Spring onset	20	3818.569	5.797985
RWIt-1 + ROS + site + T°C + RWIt-1x site	20	3818.661	5.889784
RWIt-1 + site + T°C + RWIt-1x site + Spring onset + Spring onset × site	27	3819.274	6.503368
RWIt-1 + site + T°C + RWIt-1x site + Precip. + Precip. × site	27	3819.827	7.055778
RWIt-1 + site + T°C + RWIt-1x site + Precip. + Spring onset	21	3819.941	7.170294
RWIt-1 + site + T°C + RWIt-1x site + Precip. + Snow	21	3820.008	7.237209
RWIt-1 + ROS + site + T°C + RWIt-1x site + Precip.	21	3820.145	7.373818
RWIt-1 + site + T°C + RWIt-1x site + Snow + Spring onset	21	3820.434	7.66244
RWIt-1 + ROS + site + T°C + RWIt-1x site + Snow	21	3820.491	7.719965
RWIt-1 + ROS + site + T°C + RWIt-1x site + Spring onset	21	3820.541	7.769947
RWIt-1 + ROS + site + RWIt-1x site + ROS × site	26	3823.511	10.73978
RWIt-1 + ROS + site + RWIt-1x site + ROS × site + Spring onset	27	3824.299	11.52814
RWIt-1 + ROS + site + RWIt-1x site + ROS × site + Precip.	27	3824.872	12.10084
RWIt-1 + site + T°C + RWIt-1x site +T°C × site	26	3825.244	12.47299
RWIt-1 + ROS + site + RWIt-1x site + ROS × site + Snow	27	3825.262	12.49092
RWIt-1 + site + T°C + RWIt-1x site + Snow + Snow × site	27	3826.522	13.75038
RWIt-1 + site + T°C + RWIt-1x site + Precip. + T°C × site	27	3826.747	13.97606
RWIt-1 + site + T°C + RWIt-1x site + Snow + T°C × site	27	3827.124	14.35329
RWIt-1 + site + T°C + RWIt-1x site + Spring onset + T°C × site	27	3827.165	14.39423
RWIt-1 + ROS + site + T°C + RWIt-1x site + Spring onset + T°C × site	27	3827.263	14.49209
RWIt-1 + site + RWIt-1x site	18	3827.695	14.92363
RWIt-1 + site + RWIt-1x site + Spring onset	19	3828.715	15.9434
RWIt-1 + site + RWIt-1x site + Precip.	19	3829.107	16.3357
RWIt-1 + site + RWIt-1x site + Spring onset + Spring onset × site	26	3829.397	16.62613
RWIt-1 + ROS + site + RWIt-1x site	19	3829.585	16.81394
RWIt-1 + site + RWIt-1x site + Snow	19	3829.616	16.84467

RWIt-1 + site + RWIt-1x site + Precip. + Spring onset	20	3829.87	17.09862
RWIt-1 + ROS + site + RWIt-1x site + Spring onset	20	3830.347	17.57628
RWIt-1 + site + RWIt-1x site + Precip. + Spring onset+ Spring onset × site	27	3830.596	17.8247
RWIt-1 + site + RWIt-1x site +Snow + Spring onset	20	3830.676	17.90483
RWIt-1 + site + RWIt-1x site + Precip. + Precip. × site	26	3830.789	18.01786
RWIt-1 + site + RWIt-1x site + Precip. + Snow	20	3831.086	18.31473
RWIt-1 + ROS + site + RWIt-1x site + Precip.	20	3831.119	18.34746
RWIt-1 + ROS + site + RWIt-1x site + Spring onset + Spring onset × site	27	3831.119	18.34775
RWIt-1 + site + RWIt-1x site + Snow + Spring onset + Spring onset × site	27	3831.388	18.6167
RWIt-1 + ROS + site + RWIt-1x site + Snow	20	3831.501	18.72985
RWIt-1 + site + RWIt-1x site + Precip. + Spring onset + Precip. × site	27	3831.558	18.78665
RWIt-1 + ROS + site + RWIt-1x site + Precip. + Spring onset	21	3831.748	18.97664
RWIt-1 + site + RWIt-1x site + Precip. + Snow + Spring onset	21	3831.887	19.11604
RWIt-1 + ROS + site + RWIt-1x site + Snow + Spring onset	21	3832.306	19.53531
RWIt-1 + site + RWIt-1x site + Precip. + Snow + Precip. × site	27	3832.772	20.00051
RWIt-1 + ROS + site + RWIt-1x site + Precip. + Precip. × site	27	3832.798	20.02711
RWIt-1 + ROS + site + RWIt-1x site + Precip. + Snow	21	3833.094	20.32268
RWIt-1 + site + T°C	5	3833.193	20.4223
RWIt-1 + site + T°C + Precip.	6	3834.85	22.07923
RWIt-1 + site + T°C + Spring onset	6	3834.999	22.22795
RWIt-1 + site + T°C + Snow	6	3835.015	22.24344
RWIt-1 + ROS + site + T°C	6	3835.194	22.4229

Table A4. List of all variants of the 'proxy model' tested, using the function 'dredge' from the R package 'MuMIn' (Barton 2013). All combinations were tested and ranked based on the parsimony principle of the corrected Akaike information criteron (AICc), using a maximum likelihood approach. RWIt-1= Previous year's RWI, WAO= Winter AO (November- April), SAO= Summer AO (June) Ice= June sea-ice extent.

Predictor	df	AICc	delta
RWIt-1	6	3463.849	0
RWIt-1 + SAO	7	3467.489	3.639946
RWIt-1 + WAO	7	3469.871	6.022226
RWIt-1 + SAO + WAO	8	3473.522	9.673017
RWIt-1 + Ice	7	3473.924	10.07489
RWIt-1 + SAO + Ice	8	3477.625	13.77657
RWIt-1 + WAO + Ice	8	3479.828	15.97978
RWIt-1 + SAO + WAO + Ice	9	3483.559	19.71064
SAO	6	3493.354	29.50536
WAO	6	3496.518	32.66916
SAO + WAO	7	3499.3	35.45139
Ice	6	3500.589	36.74031
SAO + Ice	7	3503.432	39.58362
WAO + Ice	7	3506.392	42.54304
SAO + WAO+ Ice	8	3509.288	45.43919

Table A5. Correlation matrix for the estimated weather variables at the Svalbard scale. Coefficients are reported with 95% confidence interval. T°C = July mean temperature (°C), Precip. = July precipitation sum (mm), Snow = November-April snowfall amount (mm), log(ROS) = "rain-on-snow" in November-April (mm) on the logarithmic scale, Spring onset = Julian day of spring onset.

	T°C	**Precip.**	**Spring onset**	**ROS**	**Snow**
T°C	1	.	.	.	.
	-0.19				
Precip.	[-0.44:0.08]	1	.	.	.
	-0.45	0.01			
Spring onset	[-0.64:-0.20]	[-0.26:0.28]	1	.	.
	0.09	0.20	-0.29		
ROS	[-0.19:0.35]	[-0.07:0.45]	[-0.52:-0.03]	1	
	0.08	-0.12	-0.07	0.06	
Snow	[-0.19:0.35]	[-0.38:0.16]	[-0.33:0.20]	[-0.21:0.32]	1

Table A6. Correlation matrix for the Svalbard climate proxy variables. Coefficients are reported with 95% confidence interval. WAO = Winter AO (November-April), SAO = Summer AO (June), Sea-ice = June sea-ice extent.

	WAO	**SAO**	**Sea-ice**
WAO	1	.	.
SAO	0.07 [-0.17:0.32]	1	.
Sea-ice	-0.25 [-0.54:0.09]	0.13 [-0.21:0.44]	1

Table A7. The average regional synchrony estimated from two different non-parametric approaches: from the one detailed in Appendix 1 and from the 'Sncf' function. Estimates were similar with the two methods, nonetheless, the estimates' precision was higher (i.e. narrower 95% confidence intervals) with the approach detailed in Appendix 1.

Parameter	Appendix 1 bootstrap	Bootstrap from 'Sncf'
$\overline{\boldsymbol{\rho}}$	0.241 [0.207:0.274]	0.245 [0.180:0.310]
$\overline{\boldsymbol{\rho_{res}}}$	0.186 [0.148:0.221]	0.188 [0.109:0.264]
$\overline{\boldsymbol{\rho_{diff}}}$	0.054 [0.040:0.068]	0.059 [-0.041:0.158]
$\overline{\boldsymbol{\rho_{T°C}}}$	0.492 [0.422:0.555]	0.491 [0.345:0.621]

Table A8. Correlation table between *Salix polaris* ring-width and July temperature at the Svalbard-scale, for three different standardisation and detrending methods of: 1) ring-width index as applied in the analysis presented in the main document, consisting of BAI and RCS standardization and temporal linear detrending of both ring-width index and weather variables (RWI det.); 2) temporal linear detrending of raw ring-width and weather data (Raw det.); 3) raw ring-width (Raw). *r* = Peason's correlation coefficient and 95% confidence interval; df = degree of freedom.

Detrending method	*r* (1962-2014, df=51)	*r* (1989-2014, df=24)
RWI det.	0.40 [0.15:0.61]	0.53 [0.19:0.76]
Raw det.	0.41 [0.16:0.62]	0.60 [0.28:0.80]
Raw	0.37 [0.11:0.58]	0.58 [0.25:0.79]

Table A9. Svalbard-scale parameter estimates for three different standardisation and detrending methods of *Salix polaris* ring-width: 1) ring-width index as applied in the analysis presented in the main document consisting of BAI and RCS standardization and temporal linear detrending of both ring-width index and weather variables (RWI det.); 2) temporal linear detrending of raw ring-width and weather data (Raw det.); 3) raw ring-width (Raw). Coefficient estimates, standard error and test statistics (*t*- and *P*-values) of the covariates are presented. Growth (*t-1*) = previous year's ring growth; July temperature (°C) = estimated mean regional July temperature. Estimates and standard errors are obtained with restricted maximum likelihood and given in 10^{-2}.

Detrending method	Intercept	July temperature (°C)	Growth (*t-1*)
RWI det.	-0.9 ± 2.89	20.72 ± 5.43	-14.87 ± 2.17
	(*t* = -0.31, p = 0.76)	(*t* = 3.82, p < .001)	(*t* = -6.86, p < .001)
Raw det.	-0.7 ± 1.38	10.62 ± 2.69	-0.12 ± 0.02
	(*t* = -0.49, p = 0.62)	(*t* = 4.08, p < .001)	(*t* = -5.41, p < .001)
Raw (μm)	-0.08 ± 11.09	8.90 ± 2.52	0.19 ± 0.02
	(*t* < .01, p = 0.99)	(*t* = 3.53, p < .001)	(*t* = 8.85, p < .001)

Table A10. The top-ranked models (ΔAICc < 2) for the model selection at the 'Svalbard scale' investigating for weather effects on *Salix polaris* ring growth. RWI_{t-1} = previous year's Ring-Width Index (RWI); T°C = July mean temperature (°C); Precip. = July precipitation sum (mm); Snow = November-April snowfall amount (mm): log(ROS) = 'rain-on-snow', i.e. November-April rain sum (mm) on the natural logarithmic scale; Spring onset = Julian day of estimated spring onset. Note that the model selection at the 'regional scale' had only one single model with ΔAICc < 2, which is presented in Table 2.

Rank	Intercept	RWI_{t-1}	T°C	log(ROS)	Snow	Precip.	Spring onset	df	AICc	ΔAICc
1	-9.06E-03	-0.15	0.21					5	3833.2	0.00
2	-8.85E-03	-0.15	0.21			-1.13E-03		6	3834.9	1.66
3	-8.92E-03	-0.15	0.21				-1.65E-03	6	3835.0	1.81
4	-9.32E-03	-0.15	0.21		3.51E-04			6	3835.0	1.82
5	-9.07E-03	-0.15	0.21	-2.95E-03				6	3835.2	2.00

Table A11. Effects of local weather on *Salix polaris* ring growth (RWI) at the 'local scale', i.e. for the sample sites where long-term weather data were available from a close by weather station (max. 30 km distance). For each site (four in total), we performed separate model selection based on corrected Akaike information criterion (AICc) with a full model containing the six selected weather variables and previous year's growth (RWI_{t-1}) as fixed effects, and year as random effect on the intercept. We present here the top-ranked models with ΔAICc < 2 for each four sites. Growth and covariates were detrended for the maximal overlapping time-span for each site. The weather variables in top-ranked models (ΔAICc < 2) differed between sites, but a positive effect of July mean temperature (T°C) in ring growth was present in three out of four sites. A strong negative effect of rain-on-snow (log(ROS)) on growth was detected in two sites: Ny-Ålesund and Kapp Linné. Snow accumulation (mm) had a slight positive effect on growth in Ny-Ålesund. Precipitation sum in July (Precip., mm) was also included in the top-ranked model in Semmeldalen. There was a strong negative delayed growth response in two out of four sites (Table S2). Spring onset = Julian day of spring onset; df = degree of freedom.

Area	Rank	Intercept	RWI_{t-1}	T°C	log(ROS)	Snow	Precip.	Spring onset	df	AICc	ΔAICc
Ny-Alesund (27 years)	1	3.25E-02	-0.38		-0.16	3.28E-03			6	247.60	0.00
	2	3.00E-02	-0.37		-0.17	3.17E-03	3.54E-03		7	248.60	1.06
	3	3.60E-02	-0.37	0.07	-0.15	3.30E-03			7	249.50	1.94
Kapp Linné (35 years)	1	-2.99E-02		0.32	-0.17				5	222.7	0
	2	-1.56E-02		0.31	-0.21			-1.47E-02	6	223.7	0.99
	3	-3.43E-02		0.29	-0.18	0.54E-03			6	224.6	1.84

		4	-1.76E-02		0.34	-0.18		2.26E-03		6	224.6	1.85
Hornsund	(42 years)	1	7.43E-03	-0.17	0.34					5	402.90	0.00
		2	8.04E-03	-0.16	0.36		1.59E-03			6	404.40	1.50
		3	7.35E-03	-0.17	0.34	0.06				6	404.50	1.61
		4	6.41E-03	-0.17	0.36			1.75E-03		6	404.70	1.76
		5	7.14E-03	-0.17	0.33				-4.24E-03	6	404.90	1.92
Semmeldalen	(29 years)	1	-1.17E-03	-0.09	0.18			-5.63E-03			1079.10	0.00
		2	-1.34E-04	-0.09	0.22						1079.40	0.32
		3	-5.42E-04	-0.09	0.21	0.03		-5.67E-03			1080.40	1.32
		4	-9.61E-04	-0.09	0.18			-5.65E-03	-3.05E-03		1080.60	1.51
		5	-2.07E-03	-0.09	0.19		-1.08E-03	-5.79E-03			1080.80	1.68
		6	4.67E-04	-0.09	0.25	0.03					1080.90	1.74
		7	5.87E-05	-0.09	0.21				-3.04E-03		1081.00	1.88

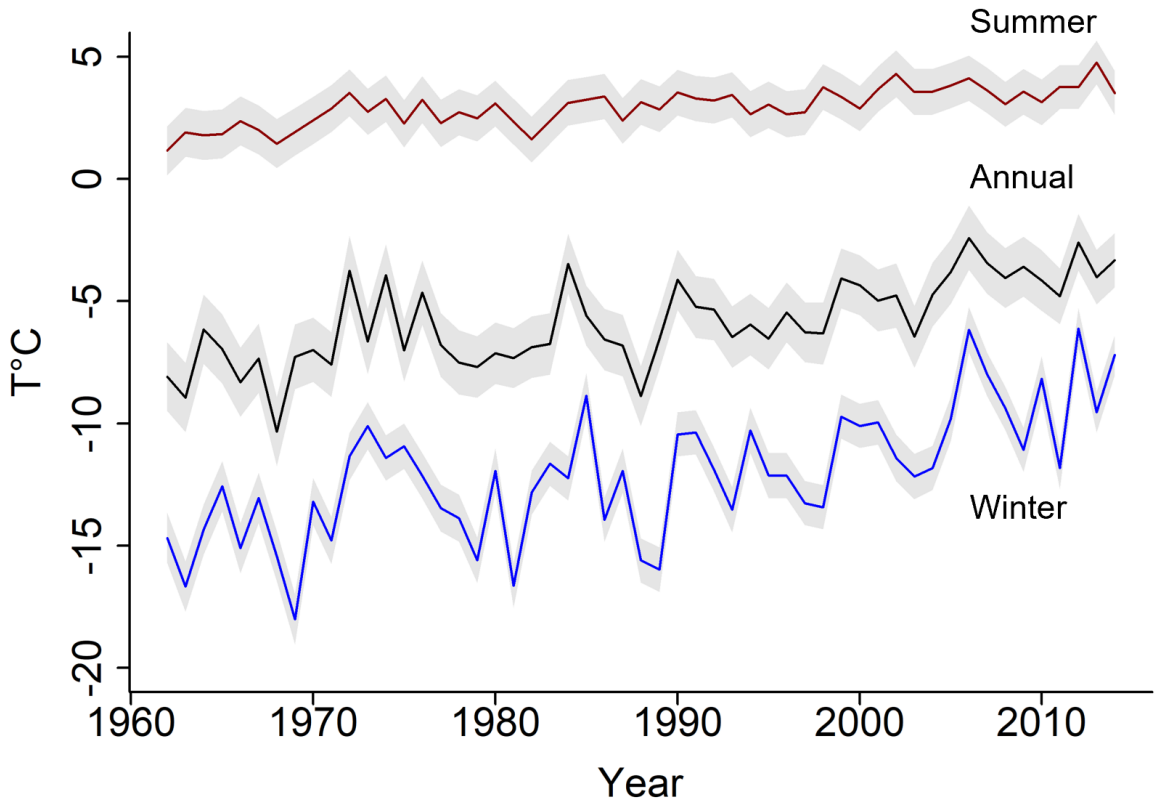

Figure A1. Temperature time-series estimated at the Svalbard-scale from models described in Methods, for the period 1962-2014. The mean annual temperature across Svalbard was -5.8 ± 0.6 (SE) °C, with winter (November [$year_{t-1}$] to April [$year_t$]) temperatures of -12.0 ± 2.6 °C and summer (June to August [$year_t$]) temperatures of 3.0 ± 0.8 °C. Mean temperature increased with a slope of 0.08 ± 0.01 (annual), 0.04 ± 0.004 (summer) and 0.11 ± 0.02 (winter) °C per year. The correlation between summer and winter temperature is r = 0.60 [0.39:0.75] (df = 51), however this is mainly due to common increasing trends. When linear detrending this temporal trend, the correlation coefficient drop to r = 0.18 [-0.10:0.43] (df = 50).

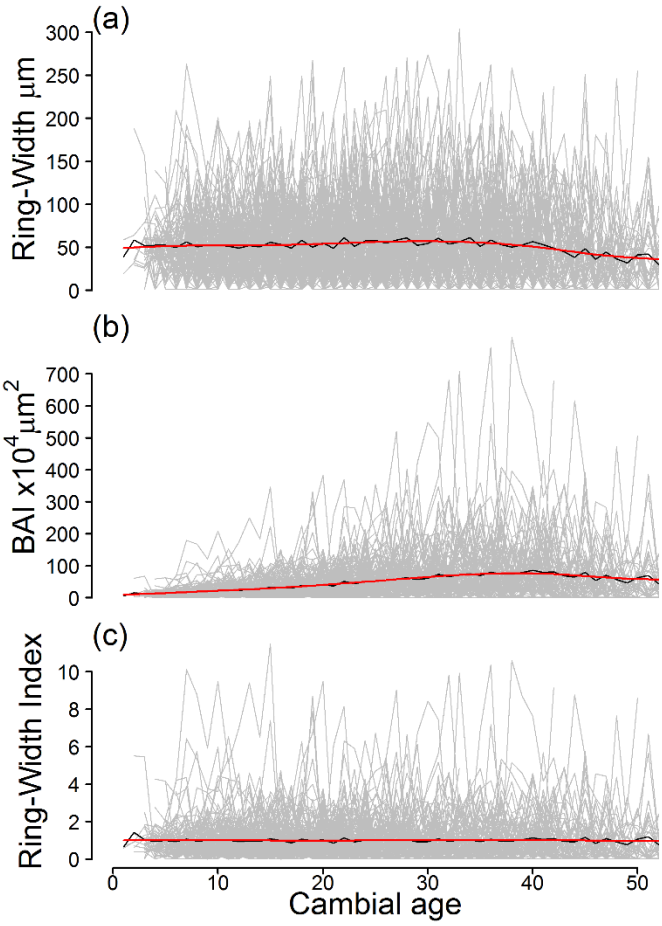

Figure A2. Age-related growth curves estimated for different standardisation steps applied to *Salix polaris* chronologies established for six study sites (i.e. without time-series from Petuniabukta and Semmeldalen, previously published in Buchwal et al. (2013) and Le Moullec et al. (2019), respectively). (a) Raw ring-width (µm) chronologies demonstrate a relatively constant growth at young age (i.e. no prominent juvenile effect). (b) Basal Area Increments (BAI in μm^2, computed from raw ring-widths) controlling for geometry. (c) BAI detrended with a regional curve standardization (RCS), removing any age-related effects and resulting in a dimensionless ring-width index measure (c) centered around 1. Note that the variance is stabilized across age. Black lines: annual mean age-related growth curve. Red curves: smoothed age-related growth trends (20 years averaged window). Grey curves: single shrubs' cross-section growth curve.

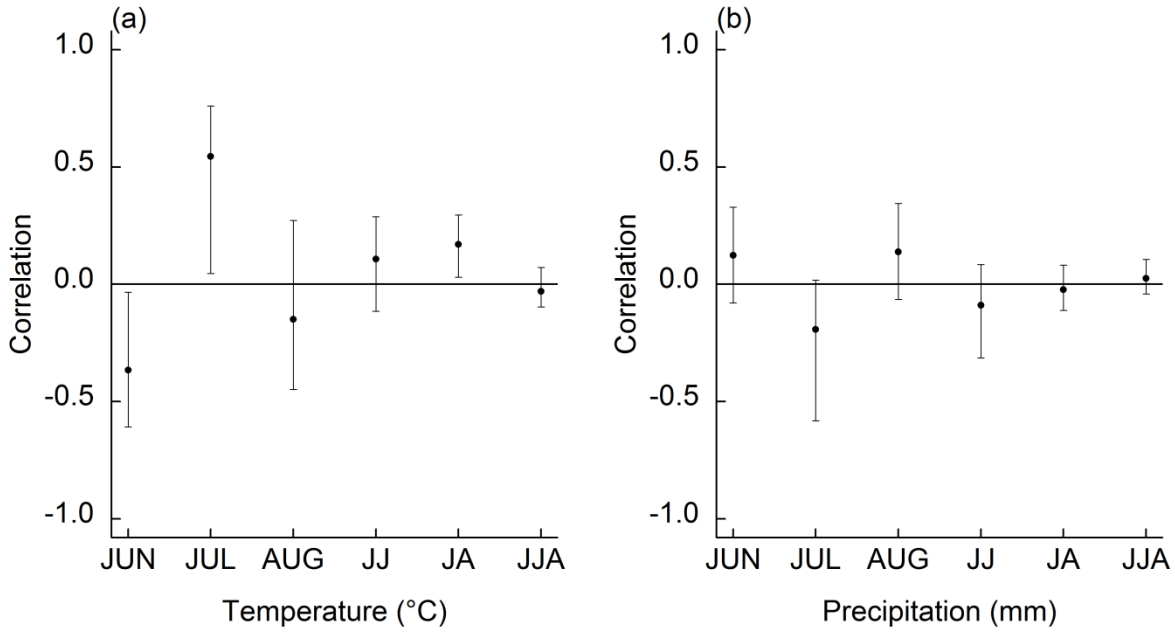

Figure A3. Pearson's correlations between *Salix polaris* ring growth (i.e. basal area increment and regional curve standardisation) in six study sites (Petuniabukta and Semmeldalen excluded) and the Svalbard scale weather variables, i.e. (a) temperature and (b) precipitation. The study period was 1989-2014, corresponding to the period of the synchrony analysis.

Figure A4. Weather variables time-series for each weather station. Black lines represent the average time-series for Svalbard.

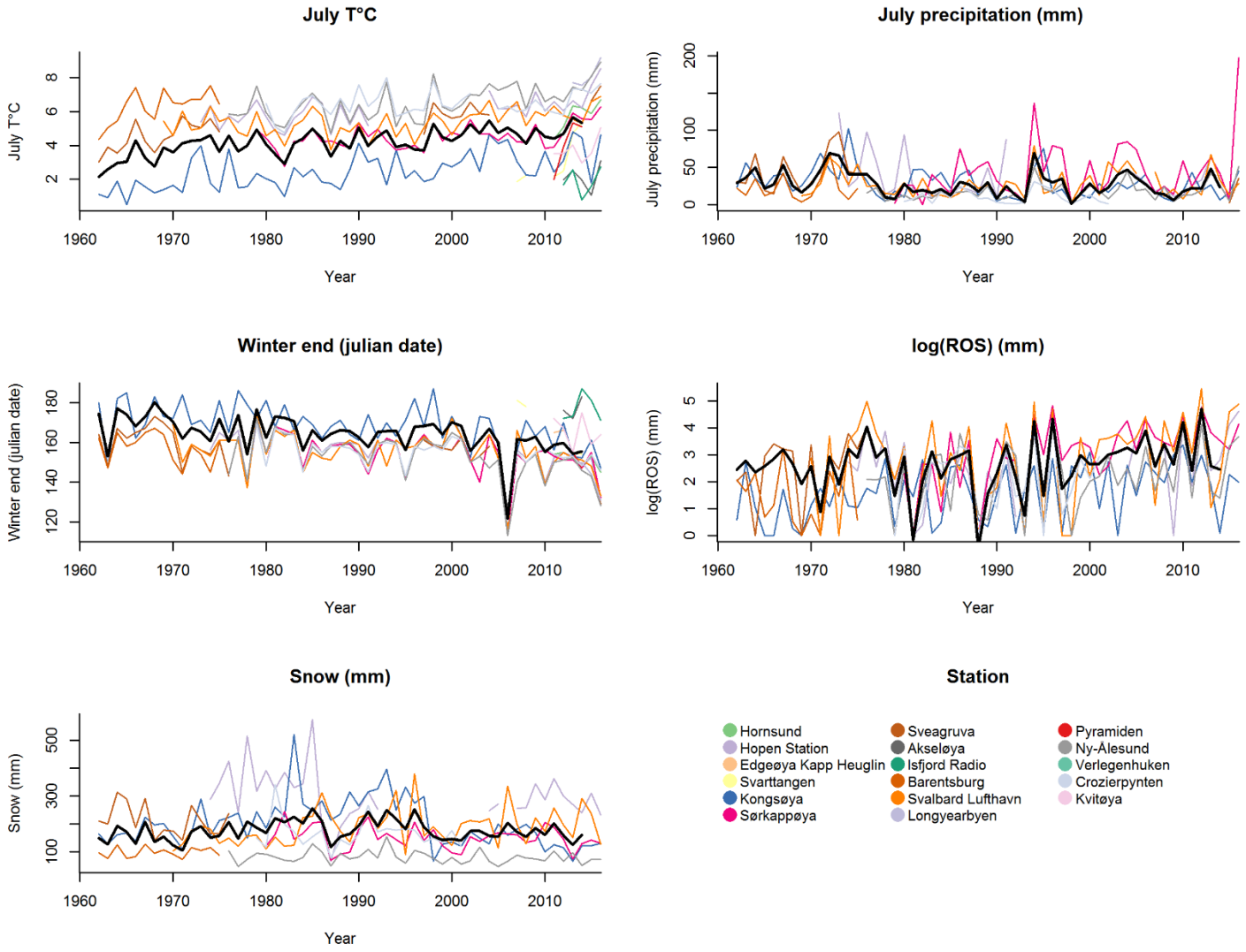

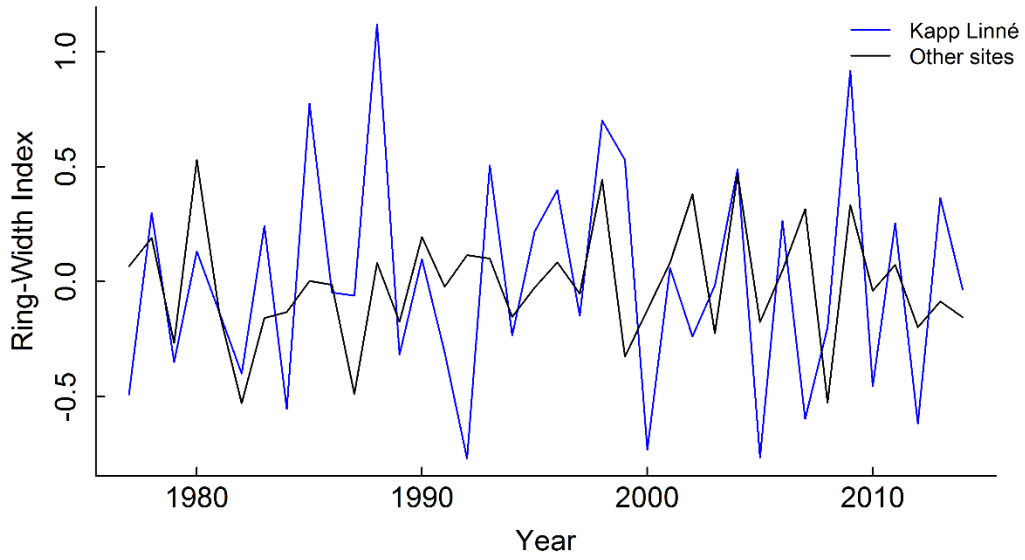

Figure A5. *Salix polaris* mean annual ring growth (ring-width index, blue line) from Kapp Linné in comparison with all other sites' mean ring growth (i.e. seven sites' average, black line). These growth curves were linearly detrended and their correlation was $r = 0.34$ [0.03:0.60] for the period 1977-2014. Despite the relatively low EPS-value for Kapp Linné, no consistent mismatch in alignment with the other Svalbard sites' mean growth curve was observed.

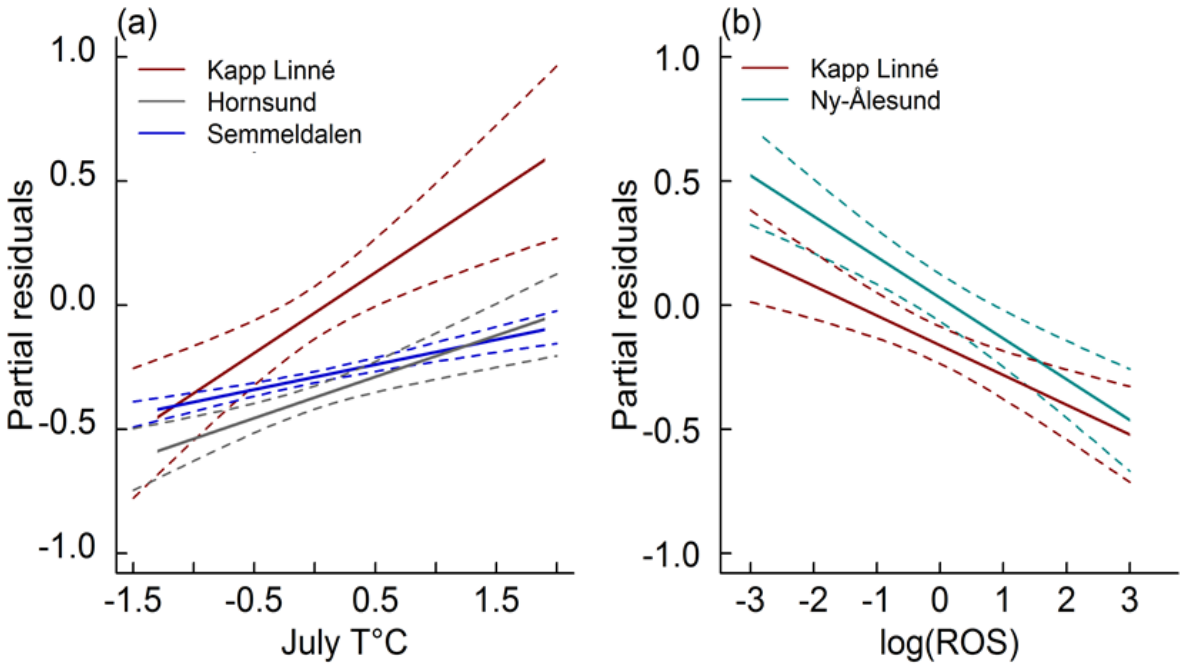

Figure A6. Partial residual plots of the effects of (a) July temperature and (b) rain-on-snow (ROS) on *Salix polaris* ring growth at the 'local scale', i.e. for the sample sites where long-term weather data were available from a close by weather station (max. 30 km distance). For each of the four locations, we used the top-ranked model presented in Table S2 to calculate the partial residuals, i.e. residuals accounting for other covariates than the one of interest ('remef' function from the R package remef, Hohenstein and Kliegl 2015). We also show the approximated 95 % confidence intervals (± 1.96 SE) as dashed lines.

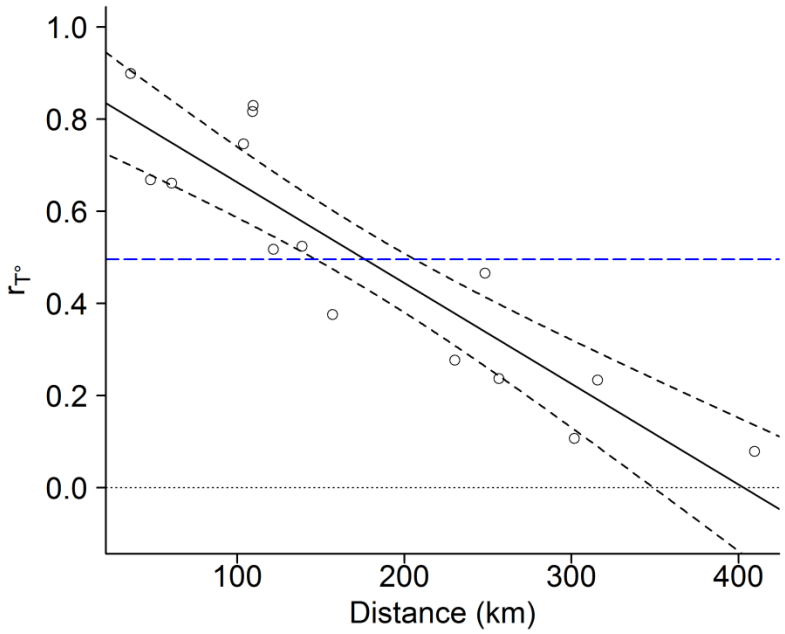

Figure A7. Spatial synchrony in July temperature across Svalbard. Pairwise Pearson's correlations (open dots) between six weather stations (1979-2014) are plotted across geographical distances (Table A1). The average regional synchrony across all distances is represented by a blue dotted line. A linear model was fitted (black solid line) with its approximate 95% confidence interval (± 1.96 SE, black dotted lines) (β intercept = 0.88 [0.77:0.99], β slope = -0.22 [-0.28:-0.17] per 100 km, R^2 = 0.81). The lower confidence interval crosses 0 at 350 km distance, which defines the spatial scale of synchrony.

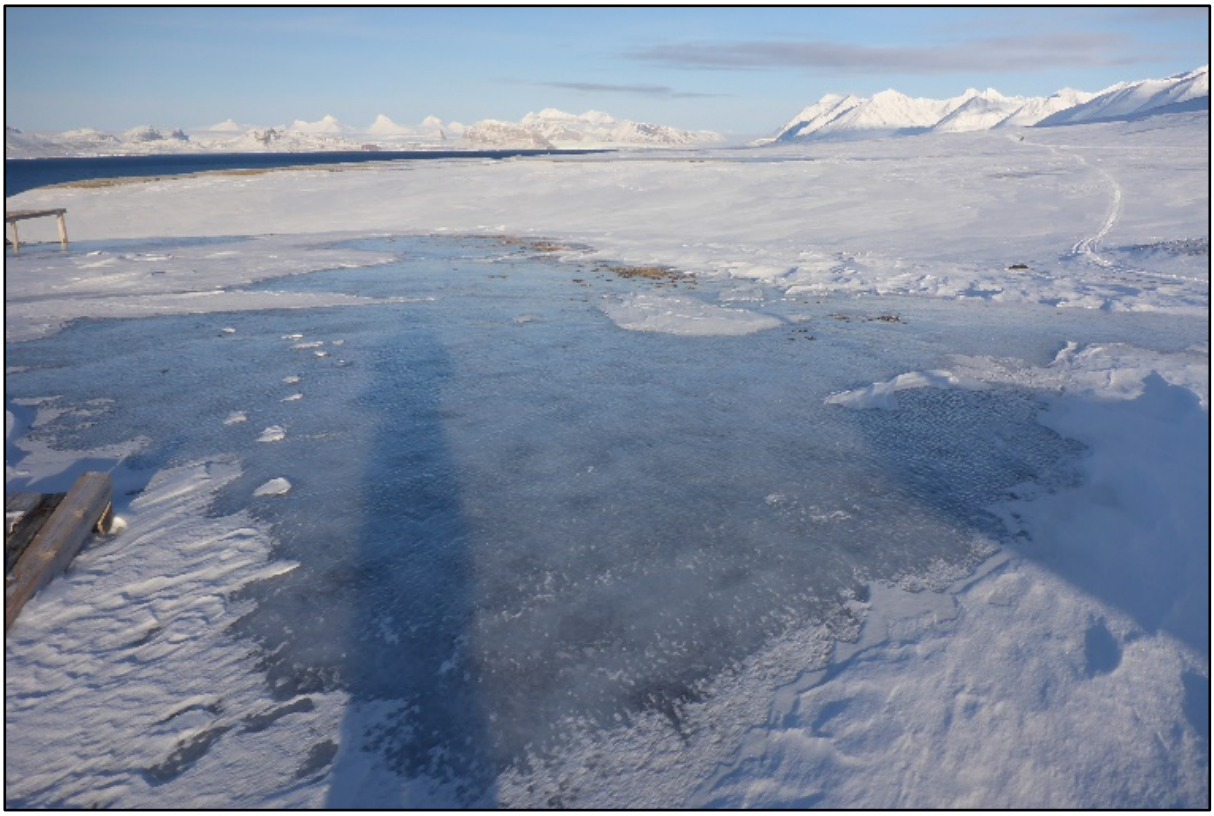

Figure A8. Continuous encasement of the vegetation in basal ice following heavy ROS in winter 2015-2016 at the collection site close to Ny-Ålesund (picture taken mid-April 2016).

References

Barton, K. 2013. MuMIn: Multi-model inference. – R package ver. 1.9.0. <https://cran.r-project.org/web/packages/MuMIn/index.html>.

Bjørnstad, O. N. 2019. ncf: spatial covariance functions. – R package ver. 1.2–8. <https://cran.r-project.org/web/packages/ncf/index.html>.

Buchwal, A. et al. 2013. Temperature modulates intra-plant growth of *Salix polaris* from a high arctic site (Svalbard). – Polar Biol. 36: 1305–1318.

Hohenstein, S. and Kliegl, R. 2015. remef: remove partial effects. – R package ver. 1.0. 6.9000. <https://github.com/hohenstein/remef>.

Le Moullec, M. et al. 2019. Annual ring growth of a widespread high-arctic shrub reflects past fluctuations in community-level plant biomass. – J. Ecol. 107: 436–451.